J. Membrane Biol. 132, 211–227 (1993)

The Journal of
Membrane Biology

Kinetics of Transient Pump Currents Generated by the (H,K)-ATPase after an ATP Concentration Jump

M. Stengelin, K. Fendler, and E. Bamberg
Max-Planck-Institut für Biophysik, W-6000 Frankfurt am Main 70, FRG

Summary. (H,K)-ATPase containing membranes from hog stomach were attached to black lipid membranes. Currents induced by an ATP concentration jump were recorded and analyzed. A sum of three exponentials ($\tau_1^{-1} \approx 400$ sec^{-1}, $\tau_2^{-1} \approx 100$ sec^{-1}, $\tau_3^{-1} \approx 10$ sec^{-1}; $T = 300$ K, pH 6, $MgCl_2$ 3 mM, no K^+) was fitted to the transient signal. The dependence of the resulting time constants and the peak current on electrolyte composition, ATP conversion rate, temperature, and membrane conductivity was recorded. The results are consistent with a reaction scheme similar to that proposed by Albers and Post for the NaK-ATPase. Based on this model the following assignments were made: τ_2 corresponds to ATP binding and exchange with caged ATP. τ_1 describes the phosphorylation reaction $E_1 \cdot ATP \rightarrow E_1P$. The third, slowest time constant τ_3 is tentatively assigned to the $E_1P \rightarrow E_2P$ transition. This is the first electrogenic step and is accelerated at high pH and by ATP via a low affinity binding site. The second electrogenic step is the transition from E_2K to E_1H. The $E_2K \leftrightarrow E_1H$ equilibrium is influenced by potassium with an apparent $K_{0.5}$ of 3 mM and by the pH. Low pH and low potassium concentration stabilize the E_1 conformation.

Key Words (H,K)-ATPase · gastric · electrogenic · concentration jump · caged ATP · black lipid membrane

Introduction

The (H,K)-ATPase from the parietal cell of the gastric mucosa transports protons in exchange for potassium ions to produce and maintain a pH level of about 1 in the mammalian stomach (*reviews:* Sachs, 1987; de Pont et al., 1988; Sachs et al., 1989; Rabon & Reuben, 1990; Wallmark, Lorentzon & Sachs, 1990). The energy for the active transport of protons against the enormous pH gradient of 6 is obtained by ATP hydrolysis. The (H,K)-ATPase belongs to the class of P-type-ATPases and has a homology in primary structure of more than 60% to the (Na,K)-ATPase (Shull, Schwarz & Lingrel, 1985). Whereas the latter one is an electrogenic pump (Thomas, 1969), the (H,K)-ATPase is electroneutral (Sachs et al., 1976). This does not imply that both potassium and proton translocation have to be electroneutral. Indeed it was shown that proton translocation is electrogenic (van der Hijden et al., 1990). There is also evidence that the K^+ limb of the cycle is potential sensitive and consequently electrogenic (Lorentzon, Sachs & Wallmark, 1988). This is different to the current model for the (Na,K)-ATPase, where most experiments suggest that the potassium step is electroneutral. However, there are also indications that this step could be electrogenic (Lafaire & Schwarz, 1986).

Based on numerous functional and structural similarities with the (Na,K)-ATPase a similar kinetic scheme for the transport mechanism (Albers, 1967; Post et al., 1969) was proposed (Sachs, 1977). An enzyme form with a high affinity for protons and a low affinity for potassium ions (E_1) binds ATP and is phosphorylated. There are at least two different phosphoenzyme forms: an ADP-sensitive and potassium-insensitive (Rabon et al., 1982) form (E_1P) and a potassium-sensitive (Ray & Forte, 1976) and ADP-insensitive form (E_2P). During the conformational change of the phosphoenzymes the proton is released to the lumen and a potassium ion is bound. Potassium stimulates dephosphorylation of E_2P yielding the E_2 form. The last step in the reaction cycle is the conformational change to E_1 with concomitant release of the potassium ion to the cytosolic side and binding of a cytosolic proton. The H^+/K^+ exchange can be described by this simple scheme; however, several modifications were proposed (Stewart, Wallmark & Sachs, 1981; Faller, Smolka & Sachs, 1985; Sachs, 1987; Reenstra, Bettencourt & Forte, 1988).

Some of the kinetic constants have been determined. Quench flow phosphorylation measurements (Wallmark & Mardh, 1979; Wallmark et al., 1980; Stewart et al., 1981; Ljungström, Vega & Mardh, 1984*b*) yielded rate constants for the ATP binding to E_1 and the phosphorylation reaction $E_1ATP \rightarrow E_1P$

under various conditions. Less is known about the $E_1P \rightarrow E_2P$ transition. The rate of the dephosphorylation $E_2P \rightarrow E_2$ is slow without potassium and saturates at 30–70 sec^{-1} for millimolar potassium depending on pH (Wallmark et al., 1980; Stewart et al., 1981). Rate constants for the reactions between E_2P and E_2 have also been determined with ^{18}O exchange measurements (Faller & Diaz, 1989). Unless the dephosphorylation is rate limiting under low potassium, the $E_2 \rightarrow E_1$ transition is probably the slowest step in the cycle (Ljungström & Mardh, 1985). Recently rate constants for this transition have been determined for the FITC-labeled enzyme (Rabon et al., 1990; Faller et al., 1991).

ATP has a high and a low affinity stimulating effect on the turnover. The high affinity binding can be assigned to ATP binding to E_1. The interpretation of the low affinity binding site is still controversially discussed. One explanation is that the E_1 and E_2 form can bind ATP, but with affinities that differ by a factor of about 1,000 (Ljungström & Mardh, 1985; Brzezinsky et al., 1988). This leads to a branched cycle between E_2 and E_1 ATP. There are, however, arguments that two ATP molecules can be bound per active enzyme complex: the molar ratio of bound vanadate to phosphoenzyme is two (Faller, Rabon, & Sachs, 1983). The same holds for the ATP analogues TNPATP (Faller, 1989) and AMPPNP (van de Ven et al., 1981). Reenstra et al., (1988) proposed that ATP can bind to a phosphoenzyme thus leading to a low affinity increase of the turnover.

It has been shown that planar lipid membranes can serve as an excellent tool to study the electrical properties of ion pumps (Drachev et al., 1974). In the case of ATP-driven pumps, membrane fragments containing the ATPase are attached to a lipid bilayer so that the systems are capacitively coupled. An ATP concentration jump via the conversion of a photolabile inactive derivative, caged ATP, induces an electrical current. This technique was applied to the Na,K-ATPase (Fendler et al., 1985; Borlinghaus, Apell, & Läuger, 1987; Nagel et al., 1987), to the Ca-ATPase (Hartung et al., 1987), and recently also to the (H,K)-ATPase (van der Hijden et al., 1990). In the latter study, it was demonstrated that parts of the reaction cycle of the (H,K)-ATPase are electrogenic. In the previous investigation of charge translocation generated by the (H,K)-ATPase, a UV lamp and a shutter with an opening time of 125 msec were used as light source for the photolysis of caged ATP. Because of the limited time resolution of this setup only the peak currents were analyzed. In the present study, a fast (≈10 nsec) laser flash enables a time resolution which is only limited by the release of ATP from caged ATP (0.29 msec at pH 6.0, 2.9 msec at pH 7.0, (McCray et al., 1980), corrected for T = 300 K with an activation energy of 55 kJ/mol (Barabas & Keszthelyi, 1984)). This allows the analysis of the electrical signal in terms of relaxation times associated with different partial reactions of the enzymatic cycle.

The behavior of the relaxation times under different conditions is discussed on the basis of a simple model for the (H,K)-ATPase reaction cycle. Assignment of the relaxation times to partial reactions is made and rate constants for some of the reactions are given and compared with the literature. In particular, the location of the electrogenic steps, an important information to elucidate the transport mechanism, is determined.

Symbols and Definitions

a_i	amplitude of an exponential component
A_i	amplitude of an exponential component obtained by the fit
C_m	specific capacitance of the black lipid membrane
C_p	specific capacitance of the adsorbed membrane
$c^0_{a,c}$	concentration of ATP/caged ATP before the laser flash
$I(t)$	measured current
$I_p(t)$	pump current of the ATPase
I_{peak}	peak current
G	measured specific conductivity of the compound membrane system
G_m	specific conductivity of the black lipid membrane
G_p	specific conductivity of the adsorbed membrane
G_{p0}	specific conductivity of the membrane without uncouplers
H^+_c, H^+_l	proton at the cytosolic/luminal site
K^+_c, K^+_l	potassium ion at the cytosolic/luminal site
k^-_x	first-order dissociation rate constant (x = H, K, etc.)
k^+_x	first-order binding rate constant
$\tilde{k}^+_x$	quasi first-order binding rate constant
k_{sat}	saturating value for k for high ATP concentrations
k_m	reciprocal membrane time constant ($\equiv G_m/C_m$)
k_0	reciprocal system time constant
$K_{0.5}$	half-saturating concentration
α	parameter that describes, how effectively uncouplers influence the conductivities of different membranes
$\lambda_{+,-}$	calculated reciprocal relaxation time
η	fraction of released ATP after flash to caged ATP before flash
τ_i	relaxation time obtained by a fit to the experimental data

Materials and Methods

Preparation of the (H,K)-ATPase

(H,K)-ATPase from pig stomach was prepared as previously described (Saccomani et al., 1977; Ljungström et al., 1984*a*) with few modifications. Mucosal scraping of the fundic part of pig

stomach was homogenized in 0.25 M sucrose. The homogenates were centrifuged at 16,000 × *g* for 30 min yielding a supernatant that was centrifuged for one hour at 31,000 × *g*. The pellet was homogenized in 0.25 M sucrose and centrifuged at 31,000 × *g* for one hour on top of a gradient consisting of 7.5% Ficoll/0.25 M sucrose over 37% sucrose. The bands at the sucrose 37%/Ficoll + sucrose and at the Ficoll + sucrose/sucrose 0.25 M interface both contain (H,K)-ATPase, but the latter one yielded higher currents on the lipid bilayer. It was diluted with distilled water and centrifuged at 30,000 × *g* for one hour. The pellet was homogenized in 0.25 M sucrose and frozen in liquid nitrogen. The activity of the preparation was 100 μM P_i mg^{-1} protein hr^{-1} (T = 37°C) and the protein concentration 10 mg/ml. The activity of the enzyme was measured with a coupled enzyme test (Albers, Koval & Siegel, 1968) and the protein content was determined according to Lowry et al. (1951).

Membrane Setup

Figure 1*A* illustrates the experimental setup. Optically black lipid membranes with an area of approximately 10^{-2} cm^2 were formed in a thermostated Teflon cell with 1.5 ml of an appropriate electrolyte solution in each compartment (Mueller et al., 1962; Bamberg et al., 1979). The membrane forming solution contained 0.3% phosphatidylserine and 1.2% phosphatidylcholine in decane (wt/vol). If not otherwise indicated, the electrolyte consisted of imidazole buffer 50 mM, $MgCl_2$ 3 mM, DTT 0.5 mM and EGTA 0.25 mM, and the temperature was 300 K. In the following sections these conditions are referred to as standard conditions. The membrane was connected to an external measuring circuit via agar-agar salt bridges and Ag/AgCl electrodes. The electrical current was amplified, filtered with a fourth order low-pass filter with a cutoff frequency of 2 kHz and recorded with a digital oscilloscope. The protein suspension (15 μl) together with 5 μl EGTA 50 mM was sonicated for 2 min with a Branson 1200 in ice-cold water and added under stirring to one side of the cuvette. Caged ATP and, if necessary, different salts from stock solutions were added under stirring to the cuvette. To photolyze caged ATP, light pulses of an excimer laser of wavelength 308 nm were attenuated by neutral density filters and focused onto the bilayer membrane. The typical energy density on the plane of the membrane was about 100 mJ/cm^2. The amount of released ATP from caged ATP was determined with a luciferin/luciferase assay. Details are described by Nagel et al. (1987). After each flash, the system was kept in the dark and stirred for at least 5 min to allow dilution of the released ATP into the cuvette volume and hydrolysis of ATP by the enzyme present in the solution. In some experiments, hexokinase together with glucose was used to speed up the ATP consumption. (For further details *see* van der Hijden et al., 1990.)

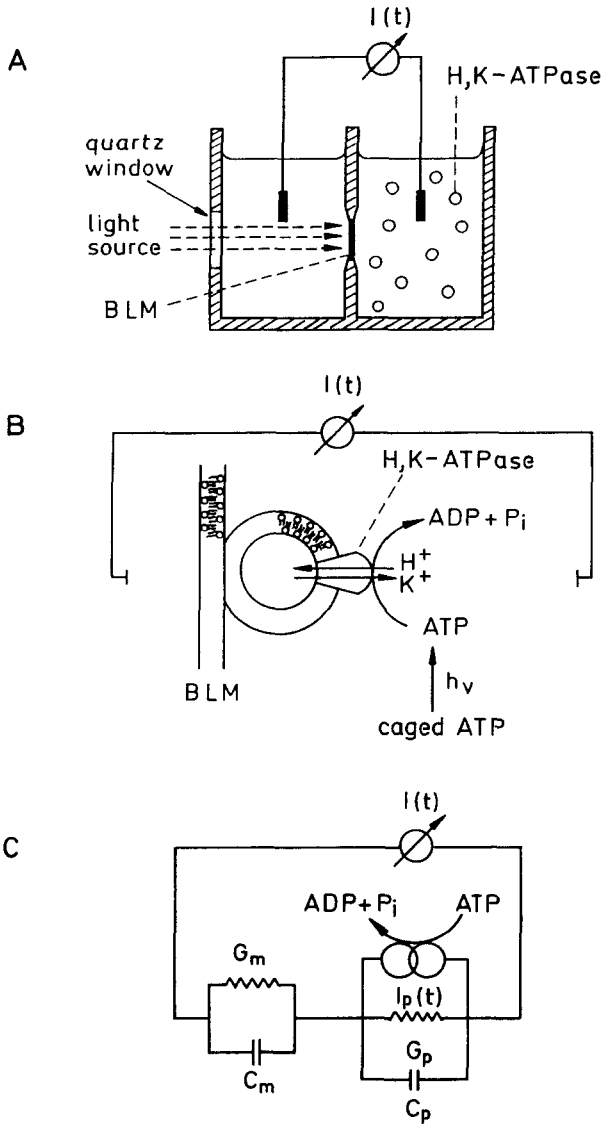

Fig. 1. Schematic representation of the bilayer setup. (*A*) Teflon cell with black lipid membrane and adsorbed H,K-ATPase vesicles. (*B*) Proposed arrangement of vesicles and underlying lipid membrane. (*C*) Equivalent circuit diagram of the two membranes in series. G_m represents the ohmic conductance of the combined parts of the black lipid membrane and adsorbed ATPase vesicles. G_p is the conductance of the residual vesicle membrane. C_m and C_p are the corresponding capacitances. I_p designates the pump current generator.

Fitting Procedure

Figure 2 shows a typical current generated by the (H,K)-ATPase after an ATP concentration jump. As for the (Na,K)-ATPase there is a fast laser artifact that does not allow using the complete signal. As indicated by the arrow the first 1–3 msec of the signal depending on the magnitude of the signal/artifact ratio were not used for the fit (*see* Fig. 2, middle panel). Curve-fitting was done with the program SPLMODD (Provencher & Vogel, 1983) that fits curves with the model function $I(t) = \sum_{i=1}^{n} A_i e^{\tau_i^{-1} t}$, where the τ_i and A_i are the adjustable fit parameters. This model function implies that the reaction cycle of the H,K-ATPase can be modeled by monomolecular or pseudomonomolecular reactions, an assumption that has been widely used in the past (Läuger et al., 1981). The model with three exponential components gave good fits in the range of three milliseconds to one second and was generally used in this study. Fits with four or five exponentials did not lead to a significantly better result. The good agreement of the fit and the data is demonstrated by the residuals shown in Fig. 2, bottom panel.

Since the first part of the signal was not used for fitting (*see arrow* in Fig. 2, middle panel), the fit curve consequently does not describe the data in this time range (Fig. 2, middle panel).

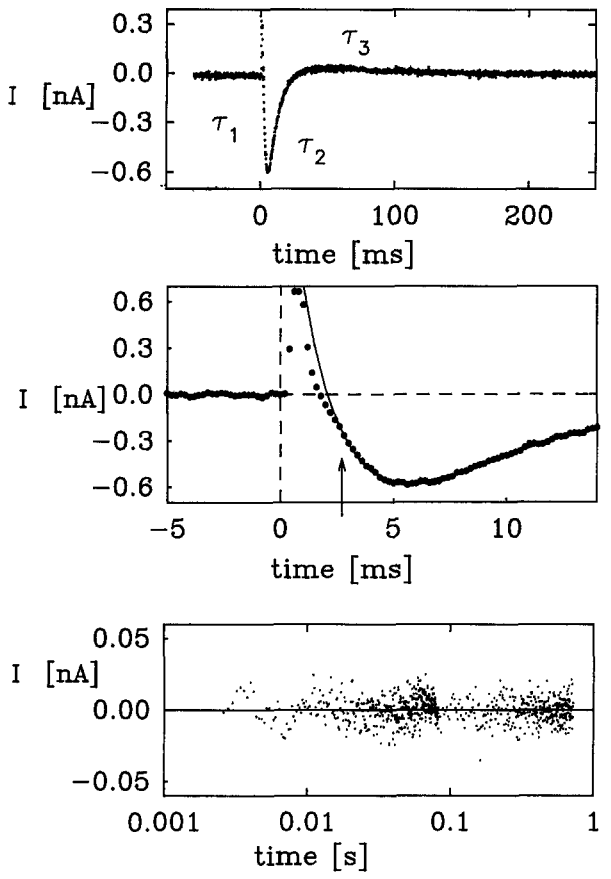

Fig. 2. Typical current signal after a UV laser flash (4,000 data points). The electrolyte contained imidazole buffer 50 mM, $MgCl_2$ 3 mM, EGTA 0.25 mM, DTT 0.5 mM, caged ATP 0.26 mM, and η = 30%. (Top panel) The signal contains at least three time constants. (Middle panel) Expanded view of the signal and the fit in the time range of the artifact. The arrow indicates where the fitted signal starts. The line is a fit with three exponentials. (Bottom panel) Residuals of the fit with three exponentials.

Time constants with $\tau^{-1} > \tau_1^{-1}$, which contribute mainly to this part of the signal, can therefore not be determined. However, the fact that the data (and the fit curve) do not extrapolate to $I = 0$ at $t = 0$ indicate that such time constants are present. Indeed, experiments with a fast amplifier (risetime $\approx$ 1 μsec, no filtering) indicate, that the signal starts at $t = 0$ with $I = 0$ and $\frac{dI}{dt} = 0$, which requires one or possibly several additional time constants with $\tau^{-1} > \tau_1^{-1}$. (Because of the reduced signal to noise ratios the fast amplifier was not used for the signals presented in this work.) The same conclusion has to be drawn from an inspection of the reaction sequence proposed for the (H,K)-ATPase in the Discussion section. In the absence of potassium, two electroneutral steps precede the electrogenic step, which also leads to a signal with $I = 0$ and $\frac{dI}{dt} = 0$ at $t = 0$. Because of the laser artifact, this phase cannot be quantitatively analyzed. Throughout this paper, this phase will be referred to as delay.

Chemicals

The protonophore 1799, the 2.6-dihydroxy-1.1.1.7.7.7.-hexafluoro-2.6.-bis-(trifluoro-methyl)heptane-4-one, was kindly provided by Dr. P.Heytler, Dupont de Nemours, Wilmington, DE. Caged ATP was prepared as described elsewhere (Kaplan, Forbush & Hoffmann, 1978; Fendler et al., 1985) and kindly provided by Dr. E. Grell, Frankfurt. Phosphatidylserine from bovine brain and synthetic diphytanoyllecitin were purchased from Avanti Lipid Products, Birmingham, AL. SCH28080 was from Byk Gulden Pharma, Konstanz. Omeprazole was a gift from Dr. B. Wallmark. Mölndal, Sweden. All other reagents were analytical or suprapure grade from Merck, Darmstadt, FRG.

Results

Addition of the (H,K)-ATPase containing membranes to one side of the cuvette and stirring for about 30 min led to adsorption of the membranes to the lipid bilayer. Release of ATP from caged ATP with a UV laser flash generated a biphasic electrical signal (*see* Fig. 2). The first phase represents the movement of a positive charge towards the protein-free compartment. The biphasic shape of the signal can be attributed to the electrical properties of the compound membrane. Several control experiments (inhibition by vanadate and omeprazole, ATP dependence, etc., van der Hijden et al., 1990) showed that the origin of the electrical signal is the (H,K)-ATPase. As a further test, we added 10 μM of the specific inhibitor SCH28080 (Beil, Hackbarth & Sewing, 1986; Scott, Sundall & Castrovilly, 1987; Wallmark et al., 1987). After 30 min the signal was reduced to 10% of its original size. Thirty minutes later it had disappeared completely (*data not shown*).

The aim of the following measurements is to associate the time constants of the electrical signal with partial reactions of the enzymatic cycle and to find which step(s) is (are) electrogenic. This can be achieved by varying several experimental conditions and observing how the signal's magnitude and form varies. The form of the signal reflects the time dependence of the concentration of the enzyme species preceding an electrogenic step (Läuger et al., 1981).

A difficulty for the interpretation of the electrical signal is the identification of the system time constant k_0^{-1} of the compound membrane that is determined by the capacitances and the conductivities of the BLM and the adsorbed membrane fragments (*see* Eq. 12). Figure 1*B* shows the arrangement of the black lipid membrane and the adsorbed membrane and Fig. 1*C* the proposed equivalent circuit. Electron microscope pictures showed that the preparation mainly consists of vesicles and a few membrane fragments. We do not know whether the elec-

trical signal is caused by membrane fragments or vesicles adsorbed to the lipid membrane. Both situations lead to the same equivalent circuit (Herrmann & Rayfield, 1978; Bamberg et al., 1979).

The conductivity of the membranes was increased by adding ionophores. In previous work (Fendler et al., 1985) the protonophore 1799 plus the $Na^+,K^+/H^+$ exchanging carrier monensin proved to be suitable.

With increasing conductivity the magnitude of the second phase of the electrical signal decreases and at conductivities of about 3 μS/cm^2 the signal becomes monophasic (van der Hijden et al., 1990). In contrast to the (Na,K)-ATPase (Fendler et al., 1985) and the Ca-ATPase (Hartung et al., 1987) there is no stationary current neither with nor without K^+, indicating that the pump operates electroneutrally under stationary conditions.

Figure 3 shows the dependence of the time constants τ_i and the amplitude a_3 of the third exponential component on the conductivity G of the compound membranes. The conductivity G was determined by applying 10 mV to the membrane and measuring the resulting current. There is no substantial conductivity dependence of the three time constants. The amplitude of the third exponential component, however, was found to vary drastically. At $G \approx 3$ μS/cm^2 a_3 vanishes and changes the sign for larger conductivities.

Alternately, to discriminate the system time constant from time constants due to the reaction cycle of the protein (protein time constants), we measured the temperature dependence between 3°C and 40°C. We expected that the system time constant has a different activation energy than the protein related time constants. Figure 4 shows the Arrhenius plot. Activation energies were 93, 67, 83 kJ/mol for $\tau_1^{-1}, \tau_2^{-1}, \tau_3^{-1}$, respectively. All three time constants showed similar activation energies. They were in the same range as those for the (Na,K)-ATPase (Fendler et al., 1992) or for the Ca-ATPase (K. Hartung, *unpublished results*).

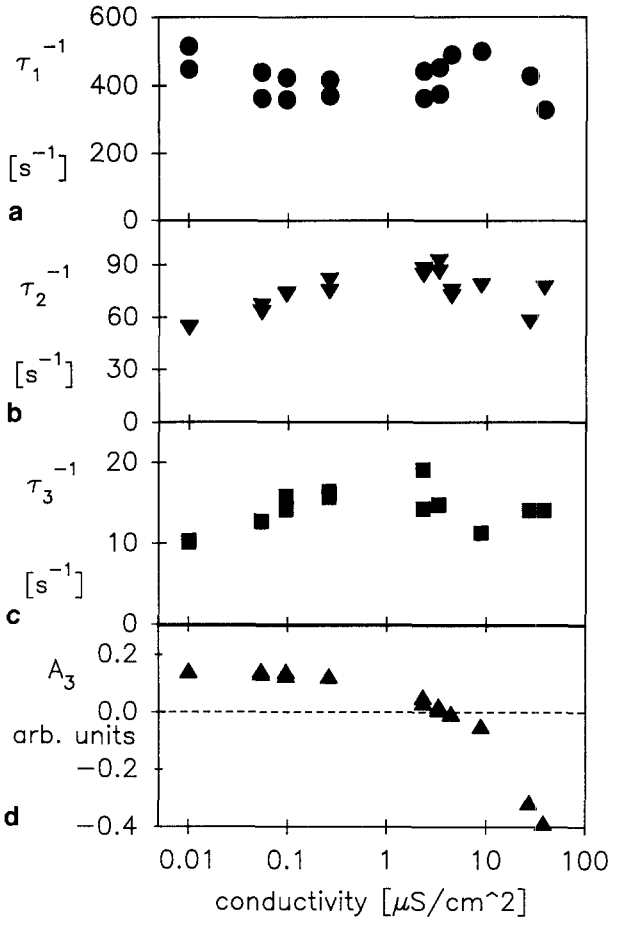

Fig. 3. Conductivity dependence of the electric signal. The electrolyte contained imidazole buffer 50 mM, pH 6.2, $MgCl_2$ 3 mM, EGTA 0.25 mM, DTT 0.5 mM, KCl 0.5 mM, glucose 50 μM, hexokinase 1 U, caged ATP 0.26 mM, η = 14%, T = 300 K. The conductivity was increased by addition of monensin and 1799. (*a–c*) show the resulting time constants of a fit with three exponentials, (*d*) the amplitude of τ_3.

ATP, Caged ATP, and ADP

Since ATP is released from caged ATP there are two possibilities to vary the ATP concentration: to change the caged ATP concentration at constant caged ATP/ATP ratio or to vary this ratio by changing the energy density of the UV light. The caged ATP concentration was successively increased from 0.8 μM to 1.5 mM. The ratio of the concentration of released ATP after a flash to the concentration of caged ATP before the flash, η, was 22%. Then η was varied in the range of 0.1 to 60% at constant caged ATP concentrations of 1.5 mM (*see* Fig. 5). The peak current, I_{peak}, increases with increasing ATP concentrations. I_{peak} is higher for identical ATP concentrations if the caged ATP concentration is lower. This indicates that caged ATP inhibits the pump. τ_1^{-1} is independent of the ATP and caged ATP concentration. τ_2^{-1} becomes faster for increasing ATP concentrations. For identical ATP concentrations τ_2^{-1} is slower if the caged ATP concentration is higher. In the discussion we will show that τ_2 describes the combined effect of ATP and caged ATP binding to E_1. τ_3^{-1} increased with increasing ATP concentrations with a $K_{0.5}$ of approximately 20 μM free ATP. No effect of caged ATP on this rate was detectable.

An interesting question is to detect an effect of ADP on the ADP-sensitive phosphoenzyme E_1P, and to examine if there is a detectable competitive

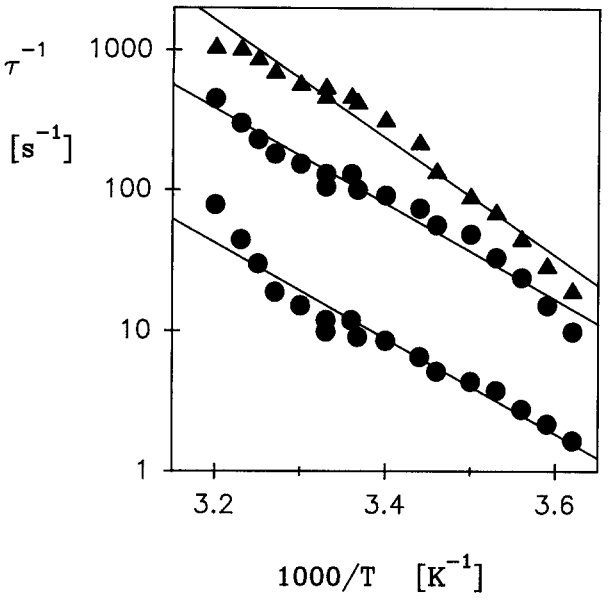

Fig. 4. Temperature dependence of the electric signal. The electrolyte contained imidazole buffer 50 mM, $MgCl_2$ 3mM, EGTA 0.25 mM, DTT 0.5 mM, caged ATP 0.26 mM, and η = 27%. The resulting activation energies were 93, 67, 83 kJ/mol for τ_1^{-1}, τ_2^{-1}, and τ_3^{-1}, respectively.

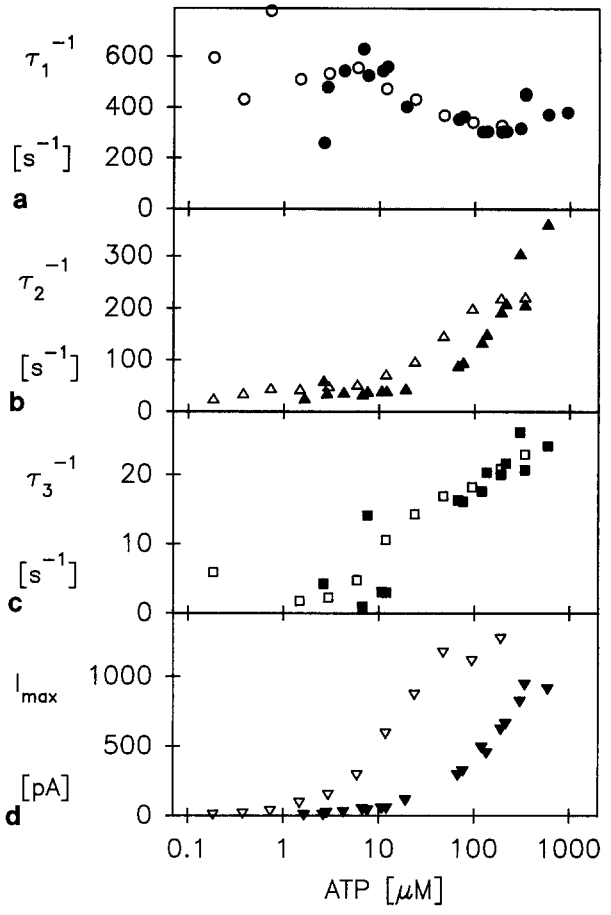

Fig. 5. ATP dependence of the electric signal. The electrolyte contained imidazole buffer 50 mM, pH 6.07, $MgCl_2$ 3 mM, EGTA 0.25 mM, DTT 0.5 mM, T = 300 K. The ATP concentration was varied in the following way: the conversion rate of caged ATP to ATP was kept at 22% and the caged ATP concentration varied (open symbols). Then the caged ATP concentration was kept constant at 1.5 mM and the conversion rate η varied by changing the laser intensity (filled symbols). (*a–c*) show the resulting time constants of a fit with three exponentials, (*d*) the peak current.

action of ADP against ATP. We measured an ADP dependence in the range of 0 to 120 μM. Figure 6 shows the effect of the ADP concentration on the form and magnitude of the electrical signal. The time constants do not change while the amplitude of the signal decreases with a $K_{0.5}$ of 60 μM.

During an experiment after each flash a fraction of caged ATP is converted into ATP and afterwards hydrolyzed yielding ADP. Therefore, a possible influence of the produced ADP on the measurements must be considered. In a typical experiment about 50 μM ATP is released from caged ATP at the membrane. The illuminated part of the solution is only about 1% of the volume. Thus, the overall concentration of released ATP is only about 0.5 μM per laser flash. Therefore, the ADP concentration produced during an experiment does not exceed 1 to 10 μM. That does not lead to a serious disturbance (*see* Fig. 6).

The Effect of Potassium and pH

As previously described (van den Hijden et al., 1990), potassium decreases the peak current with a $K_{0.5}$ of 3 mM. Figure 7 shows the potassium dependence in the range of 0 to 50 mM. In spite of the dramatic effect of potassium on the magnitude of the signal there is only a weak effect on the time constants. In the whole concentration range τ_1^{-1} does not vary substantially, whereas τ_2^{-1} and τ_3^{-1} decrease. Potassium acts not only on the cytosolic site but also on the luminal site (Stewart et al., 1981). The access of potassium to the luminal site may be restricted in our system. To test this, a potassium dependence in presence of the ionophores 1799 and monensin was measured. No substantial difference was noticed (*data not shown*).

The pH was varied by titrating the electrolyte with HCl. The peak current (*see* Fig. 8) has a maximum at pH 5.8 as shown by van den Hijden et al. (1990). The pH dependence of τ_1^{-1} is bell-shaped with a maximum at about pH 5.8. τ_2^{-1} increases monotonically between pH 5 and pH 6.5. The time constants τ_1^{-1} and τ_2^{-1} that are separated by a factor

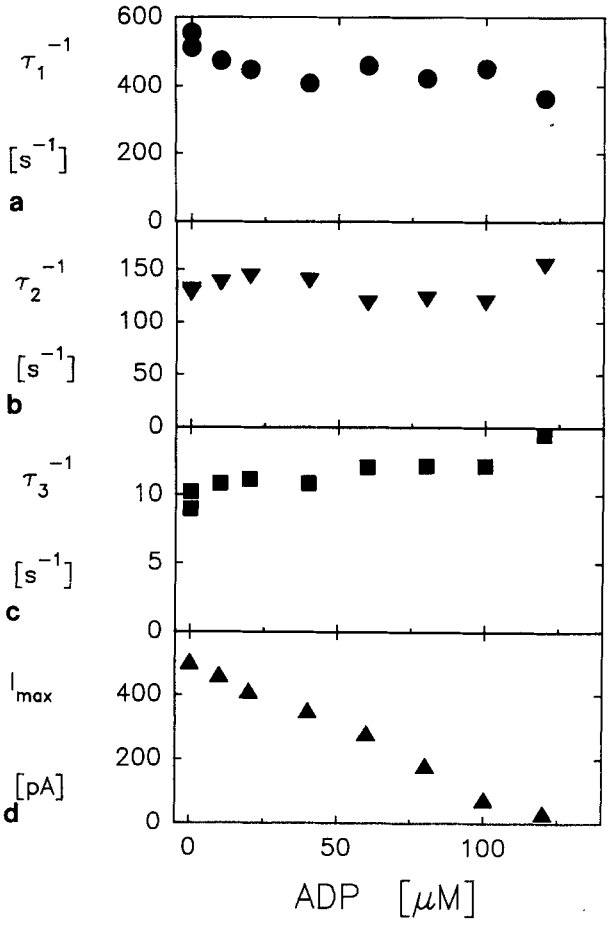

Fig. 6. ADP dependence of the electric signal. The electrolyte contained imidazole buffer 50 mM, pH 6.06, $MgCl_2$ 3 mM, EGTA 0.25 mM, DTT 0.5 mM, caged ATP 0.19 mM, η = 28%, T = 300 K. (*a–c*) show the resulting time constants of a fit with three exponentials, (*d*) the peak current.

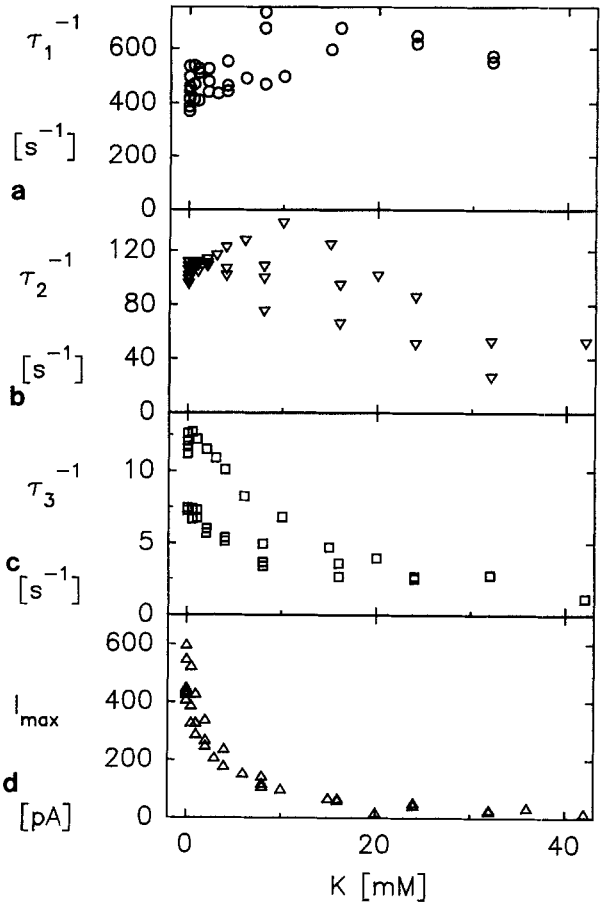

Fig. 7. K^+ dependence of the electric signal. The figure summarizes three measurements under nearly identical conditions. The electrolyte contained imidazole buffer 50 mM, pH 6.08, $MgCl_2$ 3 mM, EGTA 0.25 mM, DTT 0.5 mM, caged ATP 0.19 mM, η = 22%/28%, T = 300 K. (*a–c*) show the resulting time constants of a fit with three exponentials, (*d*) the peak current.

of about four at pH 5.8 show an opposite pH dependence and cannot be distinguished at about pH 6.5–7. τ_3^{-1} increases with increasing pH.

Discussion

To facilitate comprehension of the following subsections, a preliminary assignment of the measured relaxation times to the enzymatic partial reactions is presented. The basis for the following considerations is the Albers-Post-like reaction cycle (shown in Fig. 11). As previously demonstrated the signal consists of three time constants $\tau_1^{-1} \approx 400$ sec^{-1}, $\tau_2^{-1} \approx 100$ sec^{-1}, $\tau_3^{-1} \approx 10$ sec^{-1} at standard conditions, and at least one faster time constant that produces the delay.

The second time constant τ_2 represents the ATP binding under the influence of caged ATP. This is demonstrated by the ATP dependence and discussed in detail in section 1 below. τ_1 corresponds to the phosphorylation reaction $E_1ATP \rightarrow E_1P$. The rate of this reaction and the pH dependence reported by Ljungström et al. (1984*b*) is in agreement with τ_1. τ_3 is too slow to correspond to a step between E_1 and E_1P, and as the step following E_2P (without potassium) is slower than τ_3, it seems appropriate to assign τ_3 to the phosphoenzyme interconversion $E_1P \rightarrow E_2P$.

The delay of the signal contains several time constants. There is one time constant related to the caged ATP/ATP exchange. Another one is caused by the conductivities and capacitances of the compound membrane system (system time constant). The photolysis of the caged ATP also produces a fast time constant (0.29 msec at pH 6.0, 2.9 msec at pH 7.0, (McCray, 1980), corrected for T = 300 K

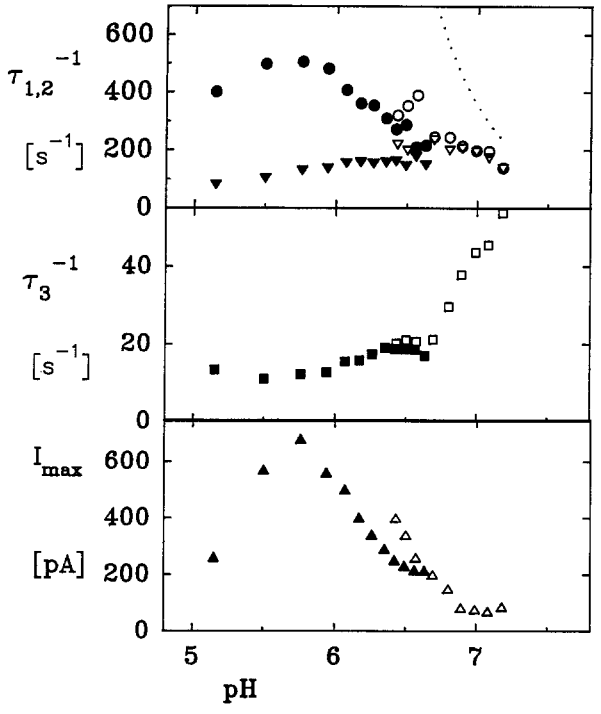

Fig. 8. PH dependence of the electric signal. The electrolyte contained imidazole buffer 50 mM, $MgCl_2$ 3 mM, EGTA 0.25 mM, DTT 0.5mM, caged ATP 0.26 mM, η = 27% T = 300 K. The solution was titrated with HCl. This figure summarizes two subsequent experiments in different pH ranges. (Top panel) shows the two fast time constants for both experiments; (Middle panel) the slow time constant τ_3^{-1} and (Bottom panel) the peak current. The dotted line in top panel is the calculated caged ATP → ATP dissociation rate according to McCray et al. (1980).

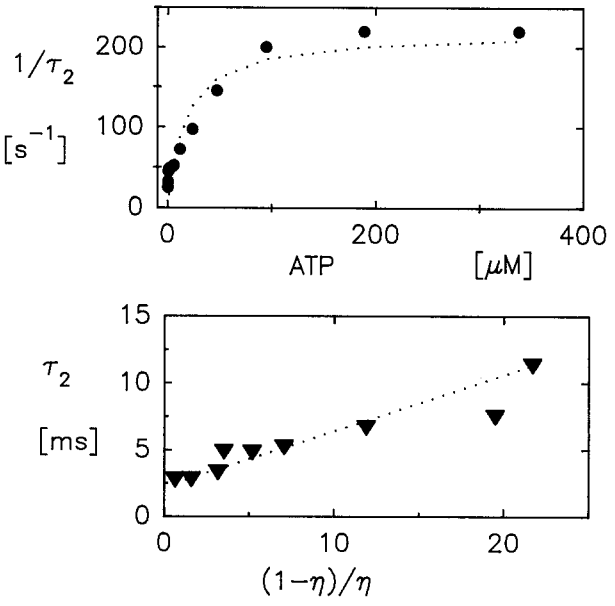

Fig. 9. Fit of the caged ATP-ATP dependence to the model described in the discussion. (Top panel) τ_2^{-1} shows a hyperbolic dependence with respect to the free ATP concentration. Fit parameters: $K_{0.5}$ = 17.5 μM, k_{sat}= 219 sec^{-1}. (Bottom panel) τ_2 is a linear function of $(1-\eta)/\eta$ with gradient 0.42 msec and intercept 2.2 msec.

with an activation energy of 55 kJ/mol (Barabas et al., 1984)) that appears in the delay. Finally, the rise time of the recording electronics (0.4–1.3 msec) contributes to the delay.

(1) τ_2 Describes the ATP Binding

For a linear reaction sequence with ATP binding, phosphorylation, and conformational change, the reciprocal relaxation time that corresponds to ATP binding should nearly proportionally increase with increasing ATP concentrations.

In contrast, a saturating behavior is observed for the ATP-dependent relaxation time constant τ_2^{-1} (Fig. 9, top panel). This can be explained by taking into account the inhibiting effect of caged ATP and can be described by the simplified reaction sequence (Fendler et al., 1992):

$$E_1\text{caged ATP} \underset{\tilde{k}_c^+}{\overset{k_c^-}{\rightleftarrows}} E_1 \xrightarrow{\tilde{k}_a^+} E_1\,\text{ATP} \rightarrow E_1P.$$

k_c^- is the caged ATP dissociation rate constant. $\tilde{k}_c^+$ and $\tilde{k}_a^+$ are the quasi first-order binding rate constants for caged ATP and ATP, respectively. They depend on the second-order rate constants k_c^+ and k_a^+:

$$\tilde{k}_a^+ \equiv k_a^+ \eta c_c^0 \quad (1)$$

$$\tilde{k}_c^+ \equiv k_c^+ (1-\eta) c_c^0 \quad (2)$$

The use of quasi first-order rate constants is justified because the concentration of ATP and caged ATP is much larger than the enzyme concentration. c_c^0 is the caged ATP concentration before the laser flash. As the rate constant of the $E_1ATP \rightarrow E_1P$ reaction is much larger ($\approx$400 sec^{-1}, *see section* 2 below) than the $E_1ATP \rightarrow E_1$ + ATP dissociation rate constant, the latter may be neglected. This uncouples the phosphorylation from the ATP/caged ATP competition reaction and the first two reactions of the scheme shown above can be treated separately. This sequence is analogous to the one treated in the Appendix and the reciprocal relaxation times can be calculated accordingly.

In the following equations, calculated reciprocal relaxation times are denoted as λ, whereas the reciprocal relaxation times obtained by a fit to experimental data are referred to as τ^{-1}.

As for the (Na,K)-ATPase it is assumed that

k_c^- and $\tilde{k}_c^+$ are fast. Then the approximation mentioned in the Appendix is justified and the reciprocal relaxation times are:

$$\lambda_- \approx \frac{k_{sat} c_c^0}{K_{0.5} + c_c^0} \tag{3}$$

$$\lambda_+ \approx \tilde{k}_c^+ + k_c^- + \tilde{k}_a^+ - \lambda_- \tag{4}$$

$$k_{sat} \equiv \eta k_a^+ K_{0.5} \tag{5}$$

$$K_{0.5} \equiv \frac{k_c^-}{k_a^+ \eta + k_c^+ (1 - \eta)} \tag{6}$$

λ_+ describes the fast caged ATP exchange and is not in an experimentally accessible range. λ_- shows at constant η a hyperbolic dependence with respect to the caged ATP concentration. If the caged ATP concentration is held constant, λ_- depends nearly linearly on η because in most cases $K_{0.5}$ depends only weakly on η. For caged ATP concentrations that are large compared to $K_{0.5}$, λ_-^{-1} is a linear function of $(1 - \eta)/\eta$:

$$\lambda_-^{-1} \approx 1/k_c^- + \frac{k_c^+ (1 - \eta)}{k_c^- k_a^+ \eta}. \tag{7}$$

The measured reciprocal time constant τ_2^{-1} is in accordance with λ_-. Using Eqs. (1) to (7) it was possible to evaluate the model parameters k_a^+, k_c^+, and k_c^-. Figure 9 (top panel) shows the hyperbolic dependence of τ_2^{-1} on the free ATP concentration as described by Eq. (3). The parameters are $k_{sat} = 219$ sec^{-1} and $\eta \cdot K_{0.5} = 17.5$ μM.

With Eqs. (3), (5), and (6) this leads to $k_a^+ \approx 12.5 \cdot 10^6$ sec^{-1} M^{-1}. The mean value for k_a^+ from four measurements was $8.3 \cdot 10^6$ sec^{-1} M^{-1}.

Figure 9 (bottom panel) together with Eq. (7) allows calculation of k_c^+ and k_c^-. There is a linear relationship between τ_2 and $(1 - \eta)/\eta$ with gradient m = 0.42 msec and intercept $\Delta y = 2.2$ msec. This leads to $k_c^- \approx 450$ sec^{-1} and $k_c^+ \approx 2.6 \cdot 10^6$ sec^{-1} M^{-1}.

Mean values out of four experiments were $k_c^- = 380$ sec^{-1} and $k_c^+ = 1.7 \cdot 10^6$ sec^{-1} M^{-1}. This leads to an affinity for caged ATP of about 220 μM.

These values may now be used to calculate the other time constant λ_+. This time constant is indeed fast ($\approx$1,000 sec^{-1} for 260 μM caged ATP and η = 20%) and cannot be resolved.

It might be of interest to compare the kinetic constants obtained by other methods with ours. Brzezinski et al (1988) used for their simulations a k_a^+ of $13 \cdot 10^6$ sec^{-1} M^{-1} for pH 7.4 and 21°C and found agreement with experimental data.

The results presented above can be used to calculate some apparent affinities for ATP. In section 2 below, we will show that the rate for the $E_1ATP \rightarrow E_1P$ transition is about 400 sec^{-1}. The ATP binding rate will be in the same time range for 50 μM ATP. Thus, the apparent affinity for the rate of EP formation is 50 μM. Wallmark et al. (1980) found a half-maximal phosphorylation rate of about 15 μM at pH 7.4.

To calculate the apparent affinity for the steady-state level of phosphoenzyme, the rate of dephosphorylation must be known. The dephosphorylation rate without potassium is about 0.1 sec^{-1} (calculated for T = 27°C from Stewart et al., 1981). The ATP binding rate is in the same range for about 0.01 μM ATP. Thus at 0.01 μM ATP ($\equiv K_{0.5}$) half-maximal phosphoenzyme level should be reached. Ray and Forte (1976) report a $K_{0.5}$ of 0.1 μM and Helmich de Jong et al. (1986), 0.016 μM.

The ATP dependence of the turnover is controversially discussed. Mostly two affinities are reported. Skrabanja, de Pont & Bonting, 1984, however, report only one. The phosphorylation shows a high affinity for ATP. The low affinity site may speed up the $E_2K \rightarrow E_1H$ rate (Ljungström & Mardh, 1985) or the conversion of the phosphoenzymes (Reenstra et al., 1988).

Let us consider the high affinity site. Values from the literature for the apparent affinity for ATP are 5 μM at pH 7 (Ray et al., 1976), 3.5 μM at pH 7.4 and 2.5 mM potassium (Wallmark et al., 1980), 2.5 μM at pH 6.5–7.5 and 1.35 mM potassium (Ljungström et al., 1984*b*).

The turnover at ATP concentrations that are high enough to saturate the high affinity site but low enough that the low affinity site is only weakly influenced is about 3 sec^{-1} at 2.5 mM potassium and pH 7.4 (Fig. 4 in Brzezinski et al., 1988, corrected for T = 27°C). Using our k_a^+, the ATP binding is as fast at 0.4 μM. There seems to be a contradiction between our values and published ones. A more detailed analysis of the enzymatic cycle, however, solves this problem: According to Brzezinski et al. (1988) the $E_1 \rightarrow E_2$ back reaction is fast (35 sec^{-1} at 21°C and pH 7.4) compared to the turnover. Thus, ATP binding to E_1 competes with this rate. Therefore, an apparent affinity of some μM results in accordance with values from the literature.

Taking into account the different experimental conditions (especially pH 6.1, this paper) and the scattering of the values reported in the literature, our k_a^+ agrees well with data from the literature. This indicates that the model we used to derive k_a^+ is adequate.

(2) τ_1 Corresponds to the $E_1ATP \rightarrow E_1P$ Transition

So far we have attributed τ_2^{-1} to the ATP binding. In a linear reaction scheme τ_1^{-1} must be assigned to one step between E_1ATP and the electrogenic step or to

the electrogenic step itself. Rate constants for partial reactions may be taken from the literature. Especially, the formation of the phosphoenzyme was extensively studied. Wallmark et al. (1980) demonstrated that the phosphorylation is faster if the enzyme is preincubated with ATP and then magnesium is added, compared to adding ATP and magnesium simultaneously. The reaction $E_1ATP \rightarrow E_1P$ is not possible without magnesium. Ljungström et al. (1984*b*) published an apparent rate of 130 sec^{-1} for the $E_1ATP \rightarrow E_1P$ reaction at pH 6 and 21°C. This rate constant is in the time range we can detect and must appear in our signal. Thus, we assume that τ_1^{-1} represents the phosphorylation.

Our value (about 400 sec^{-1} at 27°C corresponding to about 200 sec^{-1} at 21°C) seems to be somewhat larger than Ljungström's. A possible explanation is that they measured a two-step process: first, Mg binds to E_1ATP, and then E_1ATP is phosphorylated.

The pH dependence of the $E_1ATP \rightarrow E_1P$ rate was studied by Ljungström et al. (1984*b*). They reported a bell-shaped pH dependence similar to that found for τ_1 (*see* Fig. 8).

(3) Does τ_3 Correspond to a Partial Reaction of the Protein?

A pump current $I_p = \Sigma_i a_i e^{-k_i t}$ is distorted by the network representing the compound membrane (Fig. 1*C*) which leads to an electrical signal of the following form (Fendler et al., 1992):

$$I(t) = \frac{C_m}{C_m + C_p} \cdot \left[\sum_i (a_i' e^{-k_i t}) + a_0 e^{-k_0 t} \right] \tag{8}$$

with

$$a_i' = a_i \frac{k_i - k_m}{k_i - k_0} \tag{9}$$

$$a_0 = (k_m - k_0) \cdot \sum_i \frac{a_i}{k_i - k_0} \tag{10}$$

$$k_m \equiv \frac{G_m}{C_m} \tag{11}$$

$$k_0 \equiv \frac{G_m + G_p}{C_m + C_p} \tag{12}$$

The protein time constants k_i are preserved but the measured amplitudes a_i' deviate from the intrinsic amplitudes a_i. In addition, there is a new time constant k_0^{-1} with amplitude a_0, the system time constant. The variation of the amplitudes can be described by two parameters k_0 and k_m of dimension sec^{-1}. They contain the specific capacitance and the specific conductivity of the black lipid membrane and the adsorbed membrane fragments.

The capacitance of the lipid membrane is about 0.38 $\mu F/cm^2$ (Benz & Läuger, 1976) and a typical value for the capacitance of a biological membrane is $C_p \approx 1$ $\mu F/cm^2$. The specific conductivity of a black lipid membrane is 5 nS/cm^2. The conductivities of biological membranes vary over a larger scale ($1–10^5$ $\mu S/cm^2$, Hille, 1984).

To simulate the conductivity dependence of k_0 and k_m after addition of uncouplers, a simple model was assumed:

$$G_m = \Delta G$$
$$G_p = G_{p0} + \alpha \cdot \Delta G \tag{13}$$

G_{p0} is the conductivity without uncouplers, ΔG the ionophore-induced conductivity, and α describes how effectively the uncouplers increase the conductivity of the adsorbed membrane compared to the black lipid membrane. The measured conductivity G is approximately ΔG if G_p is much larger than G_m or if the black lipid membrane is only partially covered with adsorbed membranes. It is assumed that at least one of these conditions holds.

Figure 10 shows the results of calculations for several parameters G_{p0} and α. We discuss three cases: τ_3 is the system time constant—the system time constant is much slower than τ_3—the system time constant is faster than τ_1.

If $\tau_3 \approx 10$ sec^{-1} is the system time constant, then G_{p0} must be about 14 $\mu S/cm^2$ (Eqs. 12 and 13). Figure 10*a* shows the conductivity dependence of k_0 with $G_{p0} = 14$ $\mu S/cm^2$ and $\alpha = 0.4$ (unbroken line) or $\alpha = 0$ (short dashes). This has to be compared with Fig. 3*c*. For small α the conductivity dependence of τ_3 is compatible with τ_3 being the system time constant.

Figure 10*b* shows the conductivity dependence of $k_m - k_0$ with $G_{p0} = 14$ $\mu S/cm^2$ and $\alpha = 0.4$ (unbroken line) or $\alpha = 0$ (short dashes). According to Eq. (10), $k_m - k_0$ is approximately proportional to the amplitude of the system time constant. Figure 10*b* has to be compared with Fig. 3*d*. The conductivity dependence of the amplitude of the third exponential component is in accordance with the assumption that this (τ_3) is the system time constant.

Let us next consider the possibility that the system time constant is slow (≤ 1 sec^{-1}) without uncouplers. A slow time constant has a low amplitude and may not be resolved. If, however, the conductivity increases, k_0 gets faster and should appear in the signal. Figure 10*a*, long dashed line, shows the conductivity dependence of a k_0 with $G_{p0} = 0.7$ $\mu S/cm^2$ and $\alpha = 0$. For a higher α the curvature of $k_0(G)$ will be larger. A smaller G_{p0} leads to a nearly identical

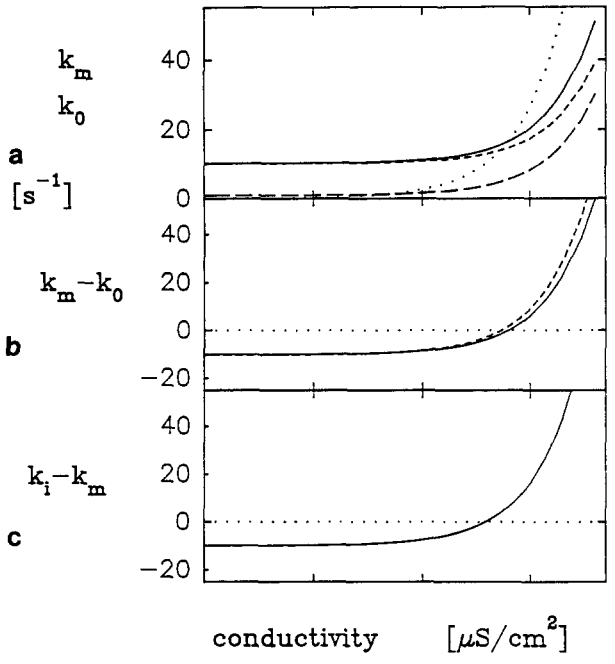

Fig. 10. Calculated conductivity dependence of k_0 and k_m. The parameters are $C_m = 0.38\ \mu F/cm^2$ and $C_p = 1\ \mu F/cm^2$. The parameters G_{p0} and α are varied to simulate that the system time constant is τ_3 (*b*); larger than τ_{1-3} (*c*); or slower than τ_3(*a*, long dashed line). (*a*) The dotted curve shows the conductivity dependence of k_m. The three other curves describe k_0 under various conditions: unbroken line, $G_{p0} = 14\ \mu S/cm^2$, $\alpha = 0.4$; short dashed line, $G_{p0} = 14\ \mu S/cm^2$, $\alpha = 0$; long dashed line, $G_{p0} = 0.7\ \mu S/cm^2$, $\alpha = 0$. (*b*) $G_{p0} = 14\ \mu S/cm^2$ and $\alpha = 0.4$ (unbroken line) or 0 (dashed line). (*c*) $k_i = 10\ sec^{-1}$.

curve. As we do not see an additional time constant up to conductivities of 30 $\mu S/cm^2$ the possibility that the system time constant is slow does not explain our data.

If the system time constant is fast (1,000 sec^{-1}) we cannot resolve it. The amplitude of a protein time constant a_i with $k_i \ll k_0$ is nearly proportional to $(k_i - k_m)$ (Eq. 9). Figure 10*c* shows $(k_i - k_m)$ for $k_i = 10$ sec^{-1}. This result is also in accordance with the amplitude of τ_3 (Fig. 3*d*).

To summarize: the conductivity dependence allows τ_3 to be the system time constant. It is also possible, however, that the system time constant is fast (1,000 sec^{-1}) and τ_3 is a protein time constant.

Equations (8–10) allow calculation of the undistorted signal if k_0 is known. In both cases the original signal is monophasic and corresponds to a movement of a positive charge towards the black lipid membrane. If τ_3 is the system time constant, then the original signal rises with τ_1 and decays with τ_2. If τ_3 is a protein time constant and $k_0 > \tau_1^{-1}$ then τ_3 describes the decay of the original signal. τ_1 corresponds to the delay (curvature = 0 for $t = 0$) and τ_2 is found in the rising phase.

In our previous study (van der Hijden et al., 1990), we proposed that τ_3 may be the system time constant. The system time constant, however, should not show any dependence on pH, potassium and ATP concentration. Also, the temperature dependence should be different for a protein time constant compared to a system time constant. Holz (1990) reported an activation energy of 20 kJ/mol for the system time constant of purple membranes and about 80 kJ/mol for protein time constants. Fendler et al. (1991), however, found activation energies of about 80 kJ/mol for protein and system time constants of electric eel membranes containing NaK-ATPase. The temperature dependence (Fig. 4) suggests that τ_3 is a protein time constant.

Also, the dependence of τ_3 on ATP concentration and pH cannot be explained under the assumption that τ_3 is the system time constant.

We cannot, however, exclude that the compound membrane system is more complex than described by the equivalent circuit (Fig. 1*C*).

Taking all arguments together, τ_3 probably corresponds to a partial reaction of the protein.

(4) τ_3 Represents the Electrogenic $E_1P \rightarrow E_2P$ Transition

In the preceding sections we have attributed τ_2 to the ATP binding and τ_1 to the phosphorylation reaction. If the reaction cycle for the (H,K)-ATPase is similar to the Albers-Post reaction scheme, τ_3 must be related to a process preceding the formation of E_1 or following the formation of E_1P. Let us consider the possibility that τ_3 describes the $E_2 \rightarrow E_1$ transition. It is possible to influence the initial conditions of the enzymatic cycle by varying the potassium concentration: low potassium induces E_1 and high potassium induces E_2 (Stewart et al., 1981, Jackson, Mendlein & Sachs, 1983; *see also* section 5 below). Thus, the amplitude a_3 of the component τ_3 should vanish for decreasing potassium concentration. This is not the case. The relation of a_1 and a_2 to a_3 varies only slightly over a large potassium concentration range.

Next we consider the possibility that τ_3 corresponds to a step following the formation of E_2P. On the basis of an Albers-Post scheme, this step is the binding of potassium and subsequent dephosphorylation. Thus, the rate and the amplitude of this step must increase with increasing potassium concentration. Without potassium the third component τ_3 should not appear in the signal. This is also not the case.

Thus, we attribute τ_3 to the $E_1P \rightarrow E_2P$ conformational change.

It is difficult to obtain values for the $E_1P \rightarrow E_2P$ rate from the literature. Helmich de Jong et al. (1985) published a rate of 1.28 min^{-1} (!) at 20°C, but this value is much too slow to be compatible with the turnover of the enzyme (9 sec^{-1} at 21°C and optimal conditions, Ljungström et al., 1984*b*). Dephosphorylation experiments with potassium showed a fast and a slow phase. The slow phase (3.5 sec^{-1} at 21°C, Wallmark et al., 1980) was interpreted as the $E_1P \rightarrow E_2P$ transition. But it seems as if this slow rate is not part of the normal catalytic cycle (Sachs, 1987; Brzezinski et al., 1988). Brzezinski et al. (1988) assumed a rate of 42 sec^{-1} at pH 7.4 and $T = 21$°C. The time constant determined in this work at comparable pH (*see* Fig. 8) is in accordance with that value.

Without potassium the dephosphorylation from E_2P is slow (≈ 0.1 sec^{-1}). An electrogenic step following E_2P thus will not appear in the transient signal. The fact that the $E_1P \rightarrow E_2P$ transition appears in the electrical signal thus requires that this step be electrogenic. (If, for example, only the phosphorylation were electrogenic we would see only τ_1 and τ_2 in the electrical signal without potassium.)

(5) The Transition from E_2 to E_1 is Slow

The (H,K)-ATPase transports both H^+ and K^+ electrogenically. Under the assumption that both ions are sequentially transported, it seems paradoxical that the electrical signal vanishes if the potassium concentration is increased. This behavior, however, can be understood on the basis of the kinetics.

Up to now we have only considered linear sequential reaction schemes. This is possible if the rate of the reaction that closes the cycle is much smaller than the other ones. In the presence of potassium it is necessary to consider a closed cycle because potassium influences the rate-limiting steps. Rate-limiting steps are the dephosphorylation for low potassium concentrations (Ray & Forte, 1976) and the $E_2 \rightarrow E_1$ transition for higher potassium concentrations (Ljungström & Mardh, 1985).

To illustrate the difference between linear sequence and closed cycle let us consider the following scheme:

$$E_2 \xrightarrow{k_1} E_1 \xrightarrow{k_2} E_1ATP \xrightarrow{k_3} E_1P \xrightarrow{k_4} E_2P \xrightarrow{k_5} E_2$$

In the case of the open cycle, k_5 is zero. For convenience let us assume that the back reactions are negligible, and the $E_1P \rightarrow E_2P$ is the only electrogenic step. The open reaction sequence has four reciprocal relaxation times $k_1, \ldots, k_4$. Let us consider the following initial conditions; (i) all enzyme molecules are in the state E_1; (ii) all enzyme molecules are in the state E_2. In the first case, the electrical signal consists of three exponentials with the reciprocal time constants k_2, k_3, k_4; in the second case, it consists of all four time constants. As the cycle is not closed, the enzyme ends in the last intermediate E_2P. This means that under both conditions the same amount of charge is transported and thus the relation $\int_{t=0}^{\infty} I(t)dt = \text{const.}$ holds. Let us assume that k_1 is much slower than all other time constants. For initial condition (ii) the signal contains the three fast time constants and, in addition, the slow one. The area under both curves is the same. Consequently, the magnitude of the peak must be much smaller in case (ii).

To summarize the case of a linear sequence: it can be explained why the peak current becomes smaller under certain initial conditions. But in this case a new time constant is introduced. We can detect time constants down to about 1 sec^{-1}. To explain the decrease of the peak current in this case, it has to be assumed that the slow preceding step has to be slower than about 1 sec^{-1}.

In the closed cycle there is one more rate constant k_5. The number of relaxation times, however, is still four. Under the assumption that k_1 is much slower than all other rates, the resulting reciprocal relaxation times are approximately k_2, k_3, k_4, k_5. This means that, independent of the initial conditions, the slow relaxation time constant k_1 does not appear in the electrical signal. But the initial conditions do influence the magnitude of the current. Again, the amplitude of the signal vanishes if all molecules start in E_2, and k_1 is much slower than the other rates.

It is known that potassium, besides its accelerating effect on dephosphorylation, also has influence on the $E_1 \rightleftharpoons E_2$ equilibrium. Potassium acts via a low affinity cytosolic site and stabilizes an E_2K form (Stewart et al., 1981, Jackson et al., 1983).

On the basis of the above considerations, the potassium dependence of the electrical signal can be understood. Without potassium, the enzyme exists before an ATP concentration jump in an E_1 state with a high affinity to ATP and the steps preceding the electrogenic step are fast. With high potassium concentration, the enzyme is in the E_2K state and the conversion to E_1H is slow compared to the other steps so that, under these initial conditions, there will be no electrical signal.

With increasing potassium concentration, the pool of enzymes that produce an electrical signal decreases, but the form of the signal does not change. This is in accordance with our experimental finding. The reason for the decrease of τ_3 with increasing potassium concentration, however, is yet

unclear. The $K_{0.5}$ for I_{peak} of 3 mM reflects the $E_1 \rightleftharpoons E_2$ equilibrium constant and may be compared with values from the literature: Rabon et al. (1990) report a $K_{0.5}$ of 5.8 mM at pH 6.4, and Helmich de Jong et al. (1986), a value of 1.3 mM at pH 7.5.

Essential for the present model is that the transition $E_2K \rightarrow E_1H$ is slow. Recently, Rabon et al. (1990) and Faller et al. (1991) measured this transition with FITC fluorescence.

Rabon et al. reported a rate constant of 18 sec^{-1} for the $E_2K \rightarrow E_1Na$ transition and of 211 sec^{-1} for the $E_1K \rightarrow E_2K$ back reaction at 20°C and pH 6.4. Faller et al. (1991) reported an even larger rate of 69 sec^{-1} for the transition $E_2K \rightarrow E_1K$ and of 118 sec^{-1} for the corresponding back reaction at 22°C and pH 7.4.

The values for the forward reactions seem to be somewhat too large to be compatible with the present model. Simulations (*not shown*) indicated an upper limit of about 10 sec^{-1} for the forward reaction rate constants. In accordance with simulations are the large rates for the back reaction.

One possible reason for the discrepancy is, that in these FITC measurements the transition not from $E_2K \rightarrow E_1H$, but $E_2K \rightarrow E_1Na$ was studied. Another possibility is that FITC itself has an influence on the measured rates.

(6) ADP Inhibits the Charge Translocation Competitively to ATP

Two possible mechanisms for the inhibition of the peak current by means of the ADP concentration were proposed (van der Hijden et al., 1990): ADP binds in competition with ATP to E_1 or ADP binds to E_1P and accelerates the back reaction. The ADP dependence of the time constants allows discrimination between both possibilities. Considering the latter case, the following simplified reaction cycle is used:

(a) Accelerating Effect of ADP on the $E_1P \rightarrow E_1ATP$ Reaction

$$\begin{array}{lll} & \overset{k^*_{ATP}}{} & \\ E_1 & \longrightarrow & E_1ATP \\ & & k_P \Downarrow\Uparrow k_{ADP} \\ & \nwarrow & \\ & & E_1P + ADP \\ & & k_e^+ \Downarrow\Uparrow k_e^- \\ & & E_2P \end{array}$$

The k's are (quasi) first-order rate constants. k^*_{ATP} takes into account the effect of ATP and caged ATP. k_{ADP} increases linearly with increasing ADP concentrations.

The decrease of the peak current may be understood under the assumption that $E_1P \rightleftharpoons E_2P$ is the electrogenic step. If, due to higher concentrations of ADP, k_{ADP} speeds up, the concentration of the intermediate E_1P decreases. As $E_1P(t)$ is proportional to the current, I_{peak} also becomes smaller.

Dephosphorylation measurements (Wallmark & Mardh, 1979) showed that, under steady-state conditions in the absence of potassium, most of the phosphoenzyme is in the E_2P conformation. This means that the back reaction $E_2P \rightarrow E_1P$ is much slower than the forward reaction and may be neglected. The dephosphorylation and conformational change $E_2P \rightarrow E_1$ without potassium is much slower than the other partial reactions. Under these assumptions the three reciprocal relaxation times for the reaction cycle are approximately k^*_{ATP}, k_P, and k_{e+} for vanishing ADP concentrations. k^*_{ATP} leads to our ATP-dependent time constant τ_2^{-1}. As shown in sections 2 and 4 above, τ_1 represents the phosphorylation and τ_3 the phosphoenzyme interconversion. Therefore, for model calculations $k^*_{ATP} = 100$ sec^{-1}, $k_P = 400$ sec^{-1}, $k_{e+} = 10$ sec^{-1}, and $k_{e-} = 0$ were used.

With increasing ADP concentrations k_{ADP} becomes faster. The effect of increasing k_{ADP} on the three reciprocal relaxation times was numerically calculated. τ_1^{-1} becomes faster, τ_2^{-1} remains nearly constant, and τ_3 gets slower. The calculations showed that a k_{ADP} which is high enough to reduce the maximal concentration of the intermediate $E_1P(t)$ (and consequently the peak current) to 50% will approximately double τ_1^{-1} and demidiate τ_3^{-1}. Comparison with Fig. 6 shows that this is not the case. Consequently, this model cannot explain our data. This does not exclude that $E_1P \rightarrow E_2P$ is the electrogenic step, but then the affinity of E_1P to ADP must be very low.

Rabon et al. (1982) could demonstrate dephosphorylation of E_1P by ADP by inhibiting the $E_1P \rightarrow E_2P$ transition with DTNB. They used 1 mM ADP. This rather low affinity of E_1P for ADP is in accordance with our finding.

(b) Competitive Action of ADP versus ATP

Next we consider the possibility that ADP competes with ATP. The following model is simplified because it does not include the effect of the caged ATP. The effect of caged ATP has to be taken into account by numerical calculations.

$$\begin{array}{lll} E_1 + ATP + ADP & \overset{k^*_{ATP}}{\longrightarrow} & E_1ATP \overset{k_P}{\longrightarrow} \\ k^+_{ADP} \Downarrow\Uparrow k^-_{ADP} & & \\ EADP & & \end{array}$$

k^*_{ATP} is an effective ATP-dependent rate constant that takes into account the effect of caged

ATP. k^+_{ADP} is the quasi first-order rate constant for ADP binding and k^-_{ADP} the EADP dissociation rate constant. k_P is the phosphorylation rate constant. As k_P is much larger than the $E_1ATP \rightarrow E_1 + ATP$ dissociation rate constant the latter one may be neglected. We can now proceed as in section 1 above and calculate the reciprocal relaxation times according to the Appendix.

The two reciprocal relaxation times are:

$$\lambda_{+,-} = \frac{k^*_{ATP} + k^-_{ADP} + k^+_{ADP}}{2} \cdot \left\{ 1 \pm \sqrt{1 - \frac{4k^-_{ADP}k^*_{ATP}}{(k^+_{ADP} + k^-_{ADP} + k^*_{ATP})^2}} \right\}. \quad (14)$$

Unless all rate constants have similar values the square root may be expanded:

$$\lambda_- \approx \frac{k^*_{ATP}k^-_{ADP}}{k^*_{ATP} + k^-_{ADP} + k^+_{ADP}} \quad (15)$$

$$\lambda_+ \approx k^+_{ADP} + k^-_{ADP} + k^*_{ATP} - \lambda_- . \quad (16)$$

Let us assume that the $E_1 \leftrightarrow$ EADP equilibrium is fast compared to k^*_{ATP}. Then λ_+ describes the fast $E_1 \leftrightarrow$ EADP equilibrium and λ_- the effect of this equilibrium on the $E_1 \rightarrow E_1ATP$ reaction.

For half-inhibiting ADP concentrations ($k^+_{ADP} = k^-_{ADP}$) Eq. (15) leads to $\lambda_- = \frac{1}{2}k^*_{ATP}$. Without ADP the reactions are uncoupled and the reciprocal relaxation time is of course equal to k^*_{ATP}. Our ATP/caged ATP dependent reciprocal time constant τ_2^{-1} corresponds in this case to λ_-. Thus, for half-inhibiting ADP concentrations τ_2^{-1} should demidiate. Comparison with Fig. 6 shows that this is obviously not the case. Therefore, this model must be discarded.

There is, however, another possibility. Let us assume that k^*_{ATP} is much larger than k^+_{ADP} and k^-_{ADP}. Then the slower reciprocal relaxation time λ_- must be related to the $E_1 \leftrightarrow$ EADP equlibrium and λ_+ corresponds to our ATP dependent time constant τ_2^{-1}.

$$\lambda_+ \approx k^*_{ATP} + k^+_{ADP} + k^-_{ADP} \cdot \left(1 - \frac{k^*_{ATP}}{k^*_{ATP} + k^-_{ADP} + k^+_{ADP}}\right). \quad (17)$$

Inspection of this equation shows that this relaxation time is indeed only weakly dependent on the ADP concentration. Numerical calculations that took into account the effect of caged ATP supported this result. Thus, it must be concluded that the ADP inhibition of the peak current is caused by a slow equilibrium between E_1 and EADP.

The slower relaxation time constant λ_- should also appear in the electrical signal. As k^*_{ATP} is large compared to k^+_{ADP}, the relation $\lambda_- \approx k^-_{ADP}$ holds. With increasing ADP concentration the ampliltude of this time constant should increase. As we do not see an additional slow time constant, we conclude that k^-_{ADP} is too slow (slower than 1 sec^{-1}) to be detected in the range of our experimental resolution. This means that both k^+_{ADP} and k^-_{ADP} are slower than the corresponding values for ATP.

(7) The Effect of the pH

It must be expected that changing the pH has complex effects not only on the transport properties of the enzyme but also rather unspecific ones.

The proton concentration affects—antagonistic to potassium—the $E_1H \rightleftharpoons E_2K$ equilibrium (Stewart et al., 1981). With decreasing pH, more enzyme molecules are in the E_1H conformation, can be phosphorylated, and produce an electrical current. This explains the pH dependence of the peak current for pH 5.8–7.

The pH dependence of τ_1^{-1} resembles the pH dependence of the reaction $E_1ATP \rightarrow EP$ as measured with phosphorylation experiments (Ljungström et al., 1984*b*).

The pH dependence of τ_2^{-1} is yet unclear. The data from Ljungström do not indicate that the ATP binding gets faster with increasing pH. So the increase of τ_2^{-1} may be explained with the caged ATP $\leftrightarrow E_1$ pre-equilibrium.

The photolysis of caged ATP is also pH dependent (McCray et al., 1980), but does not influence our signal in the observed pH range (*see* Fig. 8, top panel, dotted line).

(8) The Second Electrogenic Step is the $E_2K \leftrightarrow E_1H$ Transition

Up to now we have considered only one electrogenic step. But the lack of a steady-state current in the presence of ionophores clearly demonstrates that there is another oppositely oriented electrogenic step. An obvious candidate is the potassium translocation between E_2K and E_1H.

Let us first consider the other possibility, that the dephosphorylation $E_2P \rightarrow E_2$ is electrogenic. Without potassium, this step is rate limiting and the concentration of E_2P will be high. For millimolar potassium concentrations the dephosphorylation rate is in the range of 50 $msec^{-1}$ (Wallmark et al., 1980). Therefore, if this step were electrogenic it should appear in the electrical signal. Since no additional relaxation time is observed, it may be excluded that the dephosphorylation is electrogenic.

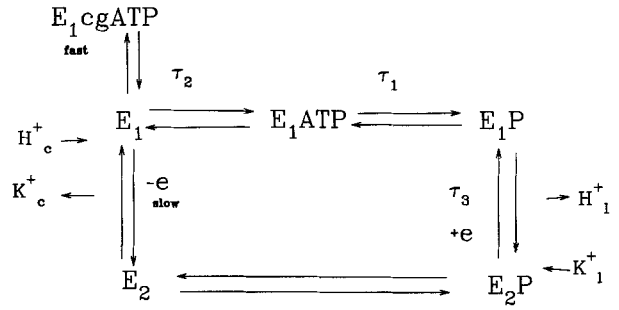

Fig. 11. Reaction scheme for the (H,K)-ATPase.

The transition from E_2K to E_1H is a two-step process: $E_2K \leftrightarrow E_1K \leftrightarrow E_1H$. Let us assume that $E_1K \leftrightarrow E_1H$ is the electrogenic step. With the initial condition that all enzymes are in E_2K this means that the signal has to start with amplitude zero. If, however, the step $E_2K \leftrightarrow E_1K$ is electrogenic, the signal has to start with a current different from zero. This means that the signal rises with the rise time of the filter. As we have a laser artifact in the same time range (*see* Figure 2, middle panel) we cannot decide which of these two possibilities holds true.

Lorentzon et al. (1988) demonstrated that the potassium limb of the reaction cycle is electrogenic in accordance with our results. As they found that the turnover is potential sensitive, the rate-limiting step under their conditions must be potential sensitive and consequently electrogenic. According to Wallmark et al. (1990) this step is the potassium release from E_1K.

Conclusions

The form and magnitude of the electrical signal after an ATP concentration jump was measured under a variety of conditions. The signal could be fitted to a sum of three exponentials. All results are in accordance with the reaction cycle shown in Fig. 11.

Before an ATP concentration jump the enzyme exists mainly in an E_1H or E_2K conformation. E_1 is preferred by low pH and low potassium concentration, whereas high pH and high potassium concentration lead to an E_2K form. The $E_2K \rightleftharpoons E_1H$ transition is slow compared to the following steps. Therefore, an enzyme molecule starting in E_2K does not produce an electrical signal. The ATP binding in the presence of the caged ATP corresponds to the ATP-dependent time constant τ_2. The fast time constant τ_1 is assigned to the reaction $E_1ATP \rightarrow E_1P$. The following conformational change $E_1P \rightarrow E_2P$ is represented by τ_3. This step is the first electrogenic step. The second electrogenic step is the transition from E_2K to E_1H. Both the dephosphorylation without potassium and the $E_2K \rightleftharpoons E_1H$ transition with potassium are rate limiting.

The authors wish to thank Dr. E. Grell and Mr. G. Schimmack. MPI Frankfurt, for synthesizing caged ATP, Mrs. S. Meister, Hoechst AG Frankfurt, for valuable help to prepare the (H,K)-ATPase, and Dr. W. Haase, MPI Frankfurt, for electron microscope pictures. (H,K)-ATPase for preliminary experiments was provided by Dr. W. Beil, Medizinische Hochschule Hannover, Dr. H. Swarts, University of Nijmegen, and Dr. G. Metzger, Hoechst AG Frankfurt. The work was supported by the Deutsche Forschungsgemeinschaft (SFB 169).

References

Albers, R.W. 1967. Biochemical aspects of active transport. *Annu. Rev. Biochem.* **36:**727–756

Albers, R.W., Koval, G.J., and Siegel, G.J. 1968. Studies on the interaction of ouabain and other cardioactive steroids with the sodium potassium activated adenosine triphosphatase. *Mol. Pharmacol.* **4:**324–336

Bamberg, E., Apell, H.J., Dencher, N.A., Sperling, W., Stieve, H., Läuger, P. 1979. Photocurrents generated by bacteriorhodopsin on planar bilayer membranes. *Biophys. Struct. Mech.* **5:**277–292

Barabas, K., Keszthelyi, L. 1984. Temperature dependence of ATP release from caged ATP. *Biochim. Biophys. Acad. Sci. Hung.* **19:**305–309

Beil, W., Hackbarth, I., Sewing, K.F. 1986. Mechanism of gastric antisecretory effect of SCH 28080. *Brit. J. Pharmacol.* **88:**19–23

Benz, R., Läuger, P. 1976. Kinetic analysis of carrier mediated ion transport: the charge pulse technique. *J. Membrane Biol.* **27:**171–191

Borlinghaus, R., Apell, H.J., Läuger, P. 1987. Fast charge translocation associated with partial reactions of the NaK Pump: I. Current and voltage transients after photochemical release of ATP. *J Membrane Biol.* **97:**169–178

Brzezinsky, P., Malmström, B.G., Lorentzon, P., Wallmark, B. 1988. The catalytic mechanism of gastric H^+/K^+-ATPase: Simulations of pre-steady-state and steady-state kinetic results. *Biochim. Biophysica Acta* **942:**215–219

de Pont, J.J.H.H.M., Helmich-de Jong, M.L., Skrabanja, A.T.P., van der Hijden, H.T.W.M. 1988. Overview: H,K-ATPase: Na,K-ATPase's stepsister. *In:* The NA,K-Pump, Part A: Molecular Aspects. J.C. Skou, J.G. Norby, A.B. Maunsbach, and M. Esmann, editors; pp. 585–602. A.R. Liss, NY

Drachev, L.A., Jasaitis, A.A., Kaulen, A.D., Kondraskin, A.A., Liberman, E.A., Nemecek. I.B., Ostroumov, S.A., Semenow, A.Y., Skulachev, V.P. 1974. The mechanism of H^+ transfer by bacteriorhodopsin direct measurement of electric current generation by cytochrome oxidase,H^+-ATPase and bacteriorhodopsin. *Nature* **249:**321–324

Faller, L.D. 1989. Competitive binding of ATP and the fluorescent substrate analogue TNP-ATP to the gasric (H,K)-ATPase: Evidence for two classes of nucleotide sites. *Biochemistry* **28:**6771–6778

Faller, L.D., Diaz, R.A., Scheiner-Bobis, G., Farley, R.A. 1991. Temperature dependence of the rates of conformational

changes reported by FITC modification of H,K- and Na,K-ATPases. *Biochemistry* **30:**3503–3510

Faller, L.D., Rabon, E., Sachs, G. 1983. Vanadate binding to the gastric (H,K)-ATPase and inhibition of the enzyme's catalytic and transport activities. *Biochemistry* **22:**4676–4685

Faller, L.D., Smolka, A., Sachs, G. 1985. The gastric H,K-ATPase. *In:* The Enzymes of Biological Membranes. A.N. Martonosi, editor. pp. 431–438. Plenum, New York/London

Faller, L.D., Diaz, R.A. 1989. Evidence from ^{18}O exchange measurements for steps involving a weak acid and a slow chemical transformation in the mechanism of phosphorylation of the gastric H,K-ATPase by inorganic phosphate. *Biochemistry* **28:**6908–6914

Fendler, K., Grell, E., Haubs, M., Bamberg, E. 1985. Pump currents generated by the purified Na^+K^+-ATPase from kidney on black lipid membranes. *EMBO J.* **4:**3079–3085

Fendler, K., Jaruschewski, S., Hobbs, A., Albers, W., Froehlich, J.P. 1992. Presteady state charge translocation in Na,K-ATPase from eel electric organ. *J. Gen. Physiol.* (*submitted*)

Hartung, K., Grell, E., Hasselbach, W., Bamberg, E. 1987. Electrical pump currents generated by the Ca-ATPase of sarcoplasmatic reticulum vesicles adsorbed on black lipid membranes. *Biochim. Biophysica Acta* **900:**209–220

Helmich de Jong, M.L., Schuurmans Stekhoven, F.M.A.H., De Pont, J.J.H.H.M. 1986. Eosin, a fluorescent marker for the high-affinity ATP site of K,H-ATPase. *Biochim. Biophysica Acta* **858:**254–262

Helmich de Jong, M.L., van Emst-de Fries, S.E., De Pont, J.J.H.H.M., Schuurmans Stekhoven, F.M.A.H., Bonting, S.L. 1985. Direct evidence for an ADP-sensitive phosphointermediate of (K^+,H^+)-ATPase, *Biochim. Biophysica Acta* **821:**377–383

Herrmann, T.R., Rayfield, T.W. 1978. The electrical response to light of bacteriorhodopsinin planar membranes. *Biophys. J.* **21:**111–125

Hille, B. 1984. Ionic Channels of Excitable Membranes; p.10. Sinauer, Sunderland, MA

Holz, M. 1990. Biophysikalische Signalanalyse mit kontinuierlichen Relaxationsspektren. VWB-Verlag, Berlin

Jackson, R.J., Mendlein, J., Sachs, G. 1983. Interaction of fluorescein isocyanate with the (H,K)-ATPase. *Biochim. Biophysica Acta* **731:**9–15

Kaplan, J.H., Forbush, B., Hoffmann, J.F. 1978. Rapid photolytic release of adenosin-5 triphosphatase from a protected analogue: utilization by the Na : K pump of human red blood cell ghosts. *Biochemistry* **17:**1925–1935

Lafaire, A.V., Schwarz, W. 1986. Voltage dependence of the threogenic NaK-ATPase in the membrane of oocytes of *Xenopus laevis*. *J. Membrane Biol.* **91:**43–51

Läuger, P., Benz, R., Stark, G., Bamberg, E., Jordan, P.C., Fahr, A., Brock, W. 1981. Relaxation studies of ion transport systems in lipid bilayer membranes. *Quarterly Rev. Biophys.* **14,4:**513–598

Ljungström, M., Mardh, S. 1985. Kinetics of the acid pump in the stomach. *J. Biol. Chem.* **260:**5440–5444

Ljungström, M., Norberg, L., Olaisson, H., Wernstedt, C., Vega, F.V., Arvidson, G., Mardh, S. 1984*a*. Characterization of proton transporting membranes from resting pig gastric mucosa. *Biochim. Biophysica Acta* **769:**209–219

Ljungström, M., Vega, F.V., Mardh, S. 1984*b*. Effects of pH on the interaction of ligands with the (H^+,K^+)-ATPase purified from pig gastric mucosa. *Biochim. Biophysica Acta* **769:**220–230

Lorentzon, P., Sachs, G., Wallmark, B. 1988. Inhibitory effects of cations on the gastric (H,K)-ATPase. *J. Biol. Chem.* **263:**10705-10710

Lowry, O.H., Rosebrough, N.J., Farr, A.L., Randall, R.J. 1951. Protein measurement with the phenol reagent. *J. Biol. Chem.* **193:**265–275

McCray, J.A., Herbette, L., Kihara, T., and Trentham, D.R. 1980. A new approach to time resolved studies of ATP requiring biological systems: laserflash photolysis of caged ATP. *Proc. Nat. Acad. Sci. USA* **77:**7237–7241

Mueller, P., Rudin, D.O., Tien, H.T., Wescott, W.C. 1962. Reconstitution of excitable cell membrane structure in vitro. *Circulation* **26:**1167–1171

Nagel, G., Fendler, K., Grell, E., Bamberg, E. 1987. Na^+ currents generated by the purified (Na^+,K^+)-ATPase on planar lipid membranes. *Biochim. Biophysica Acta* **901:**239–249

Post, R.L., Kume, S., Tobin, T., Orcutt, B., Sen, A.K. 1969. Flexibility of an active center in sodium plus potassium adenosine triphosphatase. *J. Gen. Physiol.* **54:**306–326

Provencher, S.W., Vogel, R.H. 1983. Regularisation techniques for inverse problems in molecular biology. *In:* Progress in Scientific Computing. P. Deuflhard and E. Hairer editors; pp. 304–319. Birkhaeuser, Boston

Rabon, E., Sachs, G., Mardh, S., Wallmark, B. 1982. ATP/ADP exchange activity of gastric (H^+,K^+)-ATPase. *Biochim. Biophysica Acta* **688:**515–524

Rabon, E.C., Bassilian, S., Sachs, G., Karlish, S.J.D. 1990. Conformational transitions of the H^+/K^+-atpase studied with sodium-ions as surrogates for protons. *J. Biol. Chem.* **265:**19594–19599

Rabon, E.C., Reuben, M.A. 1990. The mechanism and structure of the gastric H,K-ATPase. *Annu. Rev. Physiol.* **52:**321–344

Ray, K.T., Forte, J.G. 1976. Studies on the phosphorylated intermediates of a K^+ stimulated ATPase from rabbit gastric mucosa. *Biochim. Biophysica Acta* **443:**451–467

Reenstra, W.W., Bettencourt, J.D., Forte, J.G. 1988. Kinetic studies of the gastric H,K-ATPase. *J. Biol. Chem.* **263:**19618–19625

Saccomani, G., Stewart, H.B., Shaw, D., Lewin, M., Sachs, G. 1977. Characterization of gastric mucosal membranes: IX. Fractionation and purification of K^+-ATPase-containing vesicles by zonal centrifugation and free-flow electrophoresis technique. *Biochim Biophysica Acta* **465:**311–330

Sachs, G. 1977. H^+ transport by a nonelectrogenic gastric ATPase as a model for acid secretion. *Rev. Physiol. Biochem. Pharmacol.* **79:**133–162

Sachs, G. 1987. The gastric proton pump: the gastric H,K-ATPase. *In:* Physiology of the Gastrointestinal Tract. L.R. Johnson, editor. pp. 865–881. Raven, New York

Sachs, G., Chang, H.H., Rabon, E., Schackman, R., Lewin, M., Saccomani, G. 1976. A nonelectrogenic H^+ pump in plasma membranes of hog stomach. *J. Biol. Chem.* **251:**7690–7698

Sachs, G., Munson, K., Balaji, N., Aures-Fischer, D., Hersey, S.J., Hall, K. 1989. Functional domains of the gastric HK ATPase. *J. Bioenergetics Biomembr* **21:**573–587

Scott, C.K., Sundell, E., Castrovilly, L. 1987. Studies on the mechanism of action of the gastric microsomal (H,K)-ATPase inhibitors SCH 32651 and SCH 28080. *Biochem. Pharmacol.* **36:**97–104

Shull, G.E., Schwartz, A., Lingrel, J.B. 1985. Amino acid sequence of the catalytic subunit of the (Na^+,K^+)-ATPase deduced from a complementary DNA. *Nature* **316:**691–695

Skrabanja, A.T.P., de Pont, J.J.H.H.M., Bonting, S.L. 1984. The

H^+/ATP transport ratio of the (K,H)-ATPase of pig gastric membrane vesicles. *Biochim. Biophysica Acta* **774:**91–95

Stewart, B., Wallmark, B., Sachs, G. 1981. The interaction of H^+ and K^+ with the partial reactions of gastric (H^+K^+)-ATPase. *J. Biol. Chem.* **256:**2682–2690

Thomas, R.C. 1969. Membrane current and intracellular sodium changes in a snail neuron during extrusion of injected sodium. *J. Physiol.* **201:**495–514

van der Hijden, H.T.W.M., Grell, E., de Pont, J.J.H.H.M., Bamberg, E. 1990. Demonstration of the electrogenicity of proton translocation during the phosphorylation step in gastric (H^+,K^+)-ATPase. *J. Membrane Biol.* **114:**245–256

van de Ven, F.J.M., Schrijen, J.J., de Pont, J.J.H.H.M., Bonting, S.L. 1981. Studies on (K,H)-ATPase: III. Binding of adenyl imidodiphosphate. *Biochim. Biophysica Acta* **6340:**487–499

Wallmark, B., Briving, C., Fryklund, J., Munson, K., Jackson, R., Mendlein, J., Rabon, E., Sachs, G. 1987. Inhibition of gastric (H,K)-ATPase and acid secretion by SCH28080, a substituted pyridyl(1,2a)imidazole. *J. Biol. Chem.* **262:** 2077–2084

Wallmark, B., Lorentzon, P., Sachs, G. 1990. The gastric H^+,K^+-ATPase. *J. Internal Med.* **228:**3–8

Wallmark, B., Mardh, S. 1979. Phosphorylation and dephosphorylation kinetics of potassium-stimulated ATP phosphohydrolase from hog gastric mucosa. *J. Biol. Chem.* **254:**11899–11902

Wallmark, B., Stewart, H.B., Rabon, E., Saccomani, G., Sachs, G. 1980. The catalytic cycle of gastric (H^+,K^+)-ATPase. *J. Biol. Chem.* **255:**513–519

Received 9 March 1992; revised 28 October 1992

Appendix

Simple Two-Step Reaction Scheme

To calculate a pump current, the time dependence of the concentration(s) of the intermediate(s) preceding the electrogenic step(s) must be known (Läuger et al., 1981). For few simple reaction schemes the time dependence of the intermediates can be calculated analytically.

$$P_1 \underset{k_{2,1}}{\overset{k_{1,2}}{\rightleftharpoons}} P_2 \xrightarrow{k_{2,3}} P_3$$

This reaction scheme leads to the following differential equation system:

$$\frac{dc_1}{dt} = -k_{1,2}c_1 + k_{2,1}c_2$$

$$\frac{dc_2}{dt} = k_{1,2}c_1 + (-k_{2,1} - k_{2,3})c_2$$

$$\frac{dc_3}{dt} = k_{2,3}c_2$$

Its eigenvalues are:

$$-\lambda_{1,2} = \frac{-(k_{1,2} + k_{2,1} + k_{2,3})}{2} \cdot \left(1 \pm \sqrt{1 - \frac{4k_{1,2}k_{2,3}}{(k_{1,2} + k_{2,3} + k_{2,1})^2}}\right) \tag{A1}$$

Thus, the solution of the differential equation system is: $c_j(t) = a_{1j}e^{-\lambda_1 t} + a_{2j}e^{-\lambda_2 t}$. The a_{ij} depend on the initial conditions.

Frequently the expressions for λ may be simplified using the following approximation: $\sqrt{1-\varepsilon} \approx 1 - \frac{\varepsilon}{2}$ if $\varepsilon \ll 1$. This leads to

$$\lambda_1 \approx k_{2,3}\frac{k_{1,2}}{k_{1,2} + k_{2,3} + k_{2,1}} \tag{A2}$$

$$\lambda_2 \approx k_{1,2} + k_{2,1} + k_{2,3}\left(1 - \frac{k_{1,2}}{k_{1,2} + k_{2,3} + k_{2,1}}\right) \tag{A3}$$